

# Randomly Weighted, Untrained Neural Tensor Networks Achieve Greater Relational Expressiveness

Jinyung Hong<sup>1</sup>, Theodore P. Pavlic<sup>1,2,3</sup>

<sup>1</sup> School of Computing, Informatics, and Decision Systems Engineering, Arizona State University, Tempe, AZ 85281, USA

<sup>2</sup> School of Sustainability, Arizona State University, Tempe, AZ 85281, USA

<sup>3</sup> School of Life Sciences, Arizona State University, Tempe, AZ 85281, USA

{jhong53, tpavlic}@asu.edu

## Abstract

Neural Tensor Networks (NTNs), which are structured to encode the degree of relationship among pairs of entities, are used in Logic Tensor Networks (LTNs) to facilitate Statistical Relational Learning (SRL) in first-order logic. In this paper, we propose Randomly Weighted Tensor Networks (RWTNs), which incorporate randomly drawn, untrained tensors into an NTN encoder network with a trained decoder network. We show that RWTNs meet or surpass the performance of traditionally trained LTNs for Semantic Image Interpretation (SII) tasks that have been used as a representative example of how LTNs utilize reasoning over first-order logic to exceed the performance of solely data-driven methods. We demonstrate that RWTNs outperform LTNs for the detection of the relevant *part-of* relations between objects, and we show that RWTNs can achieve similar performance as LTNs for object classification while using fewer parameters for learning. Furthermore, we demonstrate that because the randomized weights do not depend on the data, several decoder networks can share a single NTN, giving RWTNs a unique economy of spatial scale for simultaneous classification tasks.

## Introduction

Combining knowledge-representation-and-reasoning techniques with artificial neural networks has the promise of enhancing the high performance of modern artificial intelligence (AI) with explainability and interpretability, which are necessary for generalized human insight and increased trustworthiness. Several recent studies across statistical relational learning (SRL), neural-symbolic computing, knowledge completion, and approximate inference (Koller et al. 2007; Garcez, Lamb, and Gabbay 2008; Pearl 2014; Nickel et al. 2015) have shown that neural networks can be integrated with logical systems to achieve robust learning and efficient inference as well as the interpretability provided by symbolic knowledge extraction.

These approaches to neural-network knowledge representation make use of *relational embedding*, which represents relational predicates in a neural network (Sutskever and Hinton 2009; Bordes et al. 2011; Socher et al. 2013; Santoro et al. 2017). For example, Neural Tensor Networks (NTNs)

are structured to encode the degree of relationship among pairs of entities in the form of tensor operations on real-valued vectors (Socher et al. 2013). These NTNs have been synthesized with neural symbolic integration (Garcez, Lamb, and Gabbay 2008) in the development of Logic Tensor Networks (LTNs) (Serafini and Garcez 2016), which are able to extend the power of NTNs to reason over first-order many-valued logic (Bergmann 2008).

In this paper, we propose Randomly Weighted Tensor Networks (RWTNs), a novel NTN-based network for relational embedding that incorporates randomly drawn, untrained tensors as an encoder network with a trained decoder network. Our approach is motivated by the basic architecture of an LTN combined with insights from Reservoir Computing (RC) (Jaeger 2001), which is more traditionally applied to classification problems and time-series analysis. A conventional LTN would incorporate an NTN specially trained to capture logical relationships present in data. In our case, the NTN we use is selected not by training but by drawing a 3-dimensional randomly weighted tensor acting as a generic encoder network to provide a nonlinear embedding of latent relationships among real-valued vectors. We show that a trained decoder network in RWTNs can effectively capture the likelihood of *part-of* relationships at a level of performance exceeding that of traditional LTNs even if far fewer parameters have to. Thus, even though it is untrained, the randomly drawn NTN is shown to have great relational expressiveness and acts as a general-purpose feature extractor the same way a randomly drawn recurrent reservoir in RC generates features for time-series data. To the best of our knowledge, this is the first research to integrate both RC and SRL approaches for reasoning under uncertainty and learning in the presence of data and rich knowledge. Furthermore, because the NTN weights do not depend upon the data, the single NTN network can be shared among several decoder networks each trained for a different classifier, giving RWTNs an economy of spatial scale in applications where several classifiers need to be used simultaneously.

## Related Work

RWTNs are greatly influenced by LTNs and can be viewed as a performance-based refactoring of the neural network architecture. The model theory underlying LTNs was first

proposed by Guha (2015); it represents logical terms and predicates using points/vectors in a  $n$ -dimensional real space and computes the truth value of atomic formulas by comparing the projections of the real-valued vector. By extending the theory and generalizing NTN (Socher et al. 2013), LTNs (Serafini and Garcez 2016) (and thus also RWTNs) provide more general interpretation of predicate symbols in first-order logic.

Another neural-network approach for logical representation comes from (Hybrid) Markov Logic Networks (MLNs) (Richardson and Domingos 2006; Wang and Domingos 2008; Nath and Domingos 2015). In MLNs, the number of models that satisfy a formula determines the truth value of the formula. That is, the more models there are, the higher the degree of truth. Hybrid MLNs introduce a dependency from real features associated to constants, which is given and not learned. In our model, instead, the truth value of a complex formula is determined by (fuzzy) logical reasoning, and the relations between the features of different objects is learned through error minimization.

## Preliminaries

### Reservoir Computing

Reservoir Computing (RC) is a less conventional method for using Recurrent Neural Networks that has been widely used in applications such as time-series forecasting (Dehimi and Showkati 2012; Bianchi et al. 2015b,a), process modelling (Rodan, Sheta, and Faris 2017), and classification of multivariate time series (Bianchi et al. 2018). RC models conceptually divide time-series processing into two components: (i) representation of temporal structure in the input stream through a non-adaptable dynamic *reservoir* (generated through the feedback-driven dynamics of a randomly drawn RNN), and (ii) an easy-to-adapt *readout* from the reservoir. The feedbacks within the reservoir network provide internal dynamic state variables allowing the network to re-shape and extend the duration of short patterns in time, effectively allowing the readout network to have access to “echos” of past versions of the input data. Consequently, RC techniques were originally introduced to the machine learning community under the name Echo State Networks (ESNs) (Jaeger 2001); in this paper, we use the two terms interchangeably.

The simplest formulation of the recurrent mapping from input to the internal state of the ESN is:

$$\mathbf{h}(t) = f(\mathbf{W}_{in}\mathbf{x}(t) + \mathbf{W}_r\mathbf{h}(t-1)) \quad (1)$$

where  $\mathbf{h}(t)$  is the internal state of the ESN at time  $t$ , which depends upon its previous state  $\mathbf{h}(t-1)$  and the current input  $\mathbf{x}(t)$  by way of  $f(\cdot)$ , a nonlinear activation function (usually a sigmoid or hyperbolic tangent), and the encoder parameters  $\{\mathbf{W}_{in}, \mathbf{W}_r\}$  that are randomly generated and left untrained (or implemented using a prefixed topology (Rodan and Tino 2010)). The favorable capabilities of the reservoir primarily depend on three factors: (i) a large number of processing units in the recurrent layer, (ii) random connectivity of the recurrent layer, and (iii) a spectral radius<sup>1</sup>

<sup>1</sup>The magnitude of the largest eigenvalue, which can be a rough

of the connection weights matrix  $\mathbf{W}_r$ , set to bring the system to the edge of stability (Bianchi, Livi, and Alippi 2016). Therefore, rather than training the internal weight matrices, the behavior of the reservoir can be controlled by simply modifying: the spectral radius  $\rho$ , the percentage of non-zero connections  $\beta$ , and the number of hidden units  $R$ . Another important hyperparameter is the scaling  $\omega$  of the values in  $\mathbf{W}_{in}$ , which controls the degree of nonlinearity in the processing units and, jointly with  $\rho$ , can change the internal dynamics from a chaotic system to a contractive one. Finally, for the purpose of regularization, a Gaussian noise with standard deviation  $\xi$  can be added to the state update function (Eq. (1)) as an argument (Jaeger 2001).

From the sequence of the ESN states generated over time, described by the matrix  $\mathbf{H} = [\mathbf{h}(1), \dots, \mathbf{h}(T)]^T$ , it is possible to define an encoding (representation)  $r(\mathbf{H}) = \mathbf{r}_x$  of the input sequence  $\mathbf{x}$ . Such a state becomes a vector representation with a fixed-size and can be processed by regular machine learning algorithms. Specifically, the decoder maps the input representation  $\mathbf{r}_x$  into the output space containing all class labels  $\mathbf{y}$  in a classification task:

$$\mathbf{y} = g(\mathbf{r}_x) = \mathbf{V}_o\mathbf{r}_x + \mathbf{v}_o \quad (2)$$

The decoder parameters  $\{\mathbf{V}_o, \mathbf{v}_o\}$  can be learned by minimizing a ridge regression loss function

$$\{\mathbf{V}_o, \mathbf{v}_o\}^* = \arg \min_{\{\mathbf{V}_o, \mathbf{v}_o\}} \frac{1}{2} \|\mathbf{V}_o\mathbf{r}_x + \mathbf{v}_o - \mathbf{y}\|^2 + \lambda \|\mathbf{V}_o\|^2, \quad (3)$$

which admits a closed-form solution (Scardapane and Wang 2017).

### Logic Tensor Networks

Logic Tensor Networks integrate learning based on NTNs (Socher et al. 2013) with reasoning using first-order, many-valued logic (Bergmann 2008), all implemented in TENSORFLOW<sup>TM</sup> (Serafini and Garcez 2016). This enables a range of knowledge-based tasks using rich knowledge representation in First-Order Logic (FOL) to be combined with efficient data-driven machine learning.

**First-Order Logic:** A FOL language  $\mathcal{L}$  and its signature consists of three disjoint sets— $\mathcal{C}$ ,  $\mathcal{F}$  and  $\mathcal{P}$ —denoting constants, functions and predicate symbols, respectively. For any function or predicate symbol  $s$ ,  $\alpha(s)$  can be described as its *arity*. Logical formulas in  $\mathcal{L}$  enable the description of relational knowledge. The objects being reasoned over with FOL are mapped to an interpretation domain, which is a subset of  $\mathbb{R}^n$  so that every object is associated with an  $n$ -dimensional vector of real numbers. Intuitively, this  $n$ -tuple indicates  $n$  numerical features of an object. Thus, functions are interpreted as real-valued functions, and predicates are interpreted as fuzzy relations on real vectors. With this numerical background, we can now define the numerical *grounding* of FOL with the following semantics; this grounding is necessary for NTNs to reason over logical statements.

measure of the global scaling of the weights in the case of an even eigenvalue spread.

Let  $n \in \mathbb{N}$ . An  $n$ -grounding, or simply grounding,  $\mathcal{G}$  for a FOL  $\mathcal{L}$  is a function defined on the signature of  $\mathcal{L}$  satisfying the following conditions:

- $\mathcal{G}(c) \in \mathbb{R}^n$  for every constant symbol  $c \in \mathcal{C}$ ;
- $\mathcal{G}(f) \in \mathbb{R}^{n \cdot \alpha(f)} \rightarrow \mathbb{R}^n$  for function symbol  $f \in \mathcal{F}$ ;
- $\mathcal{G}(P) \in \mathbb{R}^{n \cdot \alpha(f)} \rightarrow [0, 1]$  for predicate sym.  $P \in \mathcal{P}$ ;

Given a grounding  $\mathcal{G}$ , the semantics of closed terms and atomic formulas is defined as follows:

$$\begin{aligned} \mathcal{G}(f(t_1, \dots, t_m)) &= \mathcal{G}(f)(\mathcal{G}(t_1), \dots, \mathcal{G}(t_m)) \\ \mathcal{G}(P(t_1, \dots, t_m)) &= \mathcal{G}(P)(\mathcal{G}(t_1), \dots, \mathcal{G}(t_m)) \end{aligned}$$

According to fuzzy logic such as the Lukasiewicz  $t$ -norm (Bergmann 2008), the semantics for connectives is defined as follows:

$$\begin{aligned} \mathcal{G}(\neg\phi) &= 1 - \mathcal{G}(\phi) \\ \mathcal{G}(\phi \wedge \psi) &= \max(0, \mathcal{G}(\phi) + \mathcal{G}(\psi) - 1) \\ \mathcal{G}(\phi \vee \psi) &= \min(1, \mathcal{G}(\phi) + \mathcal{G}(\psi)) \\ \mathcal{G}(\phi \rightarrow \psi) &= \min(1, 1 - \mathcal{G}(\phi) + \mathcal{G}(\psi)) \end{aligned}$$

**Learning as Best Satisfiability:** A partial grounding  $\hat{\mathcal{G}}$  can be defined on a subset of the signature of  $\mathcal{L}$ . A grounding  $\mathcal{G}$  is said to be a completion of  $\hat{\mathcal{G}}$  if  $\mathcal{G}$  is a grounding for  $\mathcal{L}$  and coincides with  $\hat{\mathcal{G}}$  on the symbols where  $\hat{\mathcal{G}}$  is defined.

Let  $GT$  be a grounded theory which is a pair  $\langle \mathcal{K}, \hat{\mathcal{G}} \rangle$  with a set  $\mathcal{K}$  of closed formulas and a partial grounding  $\hat{\mathcal{G}}$ . A grounding  $\mathcal{G}$  satisfies a  $GT \langle \mathcal{K}, \hat{\mathcal{G}} \rangle$  if  $\mathcal{G}$  completes  $\hat{\mathcal{G}}$  and  $\mathcal{G}(\phi) = 1$  for all  $\phi \in \mathcal{K}$ . A  $GT \langle \mathcal{K}, \hat{\mathcal{G}} \rangle$  is satisfiable if there exists a grounding  $\mathcal{G}$  that satisfies  $\langle \mathcal{K}, \hat{\mathcal{G}} \rangle$ . In other words, deciding the satisfiability of  $\langle \mathcal{K}, \hat{\mathcal{G}} \rangle$  amounts to searching for a grounding  $\mathcal{G}$  such that all the formulas of  $\mathcal{K}$  are mapped to 1. Differently from classical satisfiability, when a  $GT$  is not satisfiable, we are interested in the best possible satisfaction that we can reach with a grounding. This is defined as follows. Let  $\langle \mathcal{K}, \hat{\mathcal{G}} \rangle$  be a grounded theory. We define the best satisfiability problem as the problem of finding a grounding  $\mathcal{G}^*$  that maximizes the truth values of the conjunction of all clauses  $cl \in \mathcal{K}$ , i.e.,  $\mathcal{G}^* = \arg \max_{\hat{\mathcal{G}} \subseteq \mathcal{G} \in \mathbb{G}} \mathcal{G}(\bigwedge_{cl \in \mathcal{K}} cl)$ .

**Logical Grounding and NTN:** Grounding  $\mathcal{G}^*$  captures the implicit correlation between quantitative features of objects and their categorical/relational properties. We consider groundings of the following form.

Function symbols are grounded to linear transformations. If  $f$  is a  $m$ -ary function symbol, then  $\mathcal{G}(f)$  is of the form:

$$\mathcal{G}(f)(\mathbf{v}) = M_f \mathbf{v} + N_f$$

where  $\mathbf{v} = \langle \mathbf{v}_1^\top, \dots, \mathbf{v}_m^\top \rangle^\top$  is the  $mn$ -ary vector obtained by concatenating each  $\mathbf{v}_i$ . The parameters for  $\mathcal{G}(f)$  are the  $n \times mn$  real matrix  $M_f$  and the  $n$ -vector  $N_f$ . The grounding of an  $m$ -ary predicate  $P$ , namely  $\mathcal{G}(P)$ , is defined as a generalization of the NTN (Socher et al. 2013), as a function from  $\mathbb{R}^{mn}$  to  $[0, 1]$ , as follows:

$$\mathcal{G}(P)(\mathbf{v}) = \sigma(u_P^\top \mathfrak{f}(\mathbf{v}^\top W_P^{[1:k]} \mathbf{v} + V_P \mathbf{v} + b_P)) \quad (4)$$

where  $\sigma$  is the sigmoid function and  $\mathfrak{f}$  is the hyperbolic tangent ( $\tanh$ ). The parameters for  $P$  are:  $W_P^{[1:k]}$ , a 3-D tensor in  $\mathbb{R}^{k \times mn \times mn}$ ,  $V_P \in \mathbb{R}^{k \times mn}$ ,  $b_P \in \mathbb{R}^k$  and  $u_P \in \mathbb{R}^k$ .

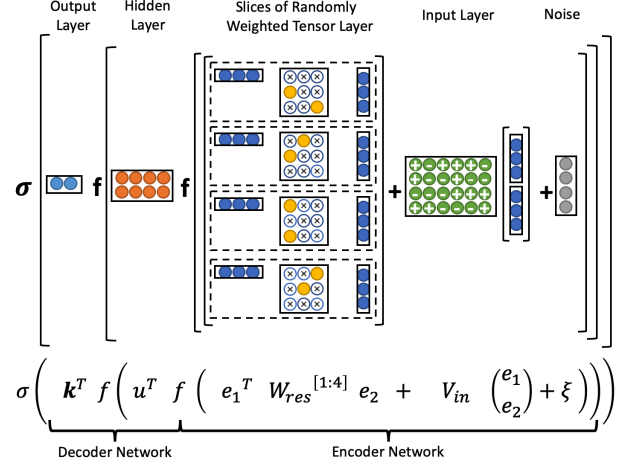


Figure 1: Visualization of the structure of the Randomly Weighted Tensor Network. Each dashed box represents one slice of the randomly weighted tensor  $W_{res}^{[1:R]}$ , in this case there are  $R = 4$  slices.

## Randomly Weighted Tensor Networks

Here, we introduce the mathematical and structural definitions of Randomly Weighted Tensor Networks (RWTNs). By combining a randomly drawn, untrained tensor into an NTN encoder network with a trained decoder network, our model has fewer parameters to learn and can also achieve greater expressive capability for extracting relational knowledge as an LTN trained for the same task.

### The Definition of RWTNs

RWTNs can be defined as a function from  $\mathbb{R}^{mn}$  to  $[0, 1]$ :

$$\mathcal{G}_{rwtN}(P)(\mathbf{v}) = \sigma(\mathbf{k}^\top \mathfrak{f}(u^\top \mathfrak{f}(\mathbf{v}^\top W_{res}^{[1:R]} \mathbf{v} + V_{in} \mathbf{v} + \xi))) \quad (5)$$

where  $\sigma$  is the sigmoid function and  $\mathfrak{f}$  is the hyperbolic tangent ( $\tanh$ ) function. The parameters of the RWTN encoder include:  $W_{res}^{[1:R]} \in \mathbb{R}^{mn \times mn \times R}$  (a 3-dimensional randomly weighted tensor),  $V_{in} \in \mathbb{R}^{R \times mn}$  (randomly drawn input-layer weights), and  $\xi$  (Gaussian noise). The parameters of the RWTN decoder are thus  $u \in \mathbb{R}^{R \times t}$  and  $\mathbf{k} \in \mathbb{R}^t$ , which are the standard weights for a single hidden layer neural network where  $t$  is the number of neurons in a hidden layer. Fig. 1 shows a sample visualization of the structure of our model.

In the depicted case,  $e_1, e_2 \in \mathbb{R}^d$  are vector representations (or features) of two entities for which the RWTN expresses some level relationship between. Each slice of the tensor  $W_{res}^{[1:R]}$  can be viewed as being responsible for representing one kind of relationship between the two entities. In principle, the network could be trained to explicitly represent certain relationships. However, this tensor is randomly weighted in RWTN to span a wide range of potential relationships that are left to the later decoder to mix to represent

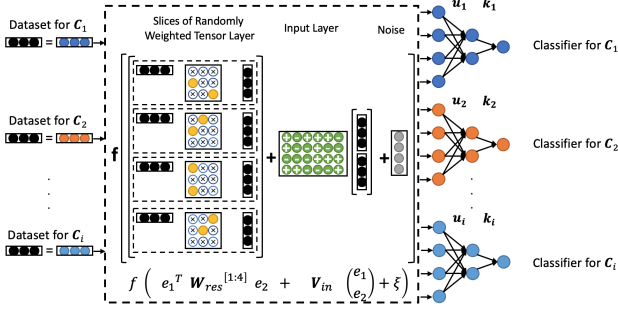


Figure 2: Visualization of the structure of the Randomly Weighted Tensor Network with weight sharing. In the case of learning each classifier from the class  $C_1$  to the class  $C_i$ , RWTNs allow us to use the same encoder network to extract features from each data from the class  $C_1$  to the class  $C_i$ .

the desired relationships from data. There are the following characteristics of our model:

- Non-adaptability of the parameters in the encoder network, inspired by the insights of Reservoir Computing (RC): the tensor  $W_{res}^{[1:R]}$  are selected to have a greater number of units, random sparsity, and a certain spectral radius. Also, the input weights  $V_{in}$  are generated randomly from a uniform distribution over an interval  $[-\omega, \omega]$  with random sign determined by a random draw from Bernoulli distribution (input-layer weights in Fig. 1). A Gaussian noise  $\xi$  is used for the same purpose of the one in RC, which is regularization. We intend that by having those properties, the randomly weighted tensor and input weights in our model can act as a filter that converts the latent relationship between objects using a high-dimensional map, similar to the operation of an explicit, temporal kernel function.
- Succinctness in learning process of a decoder network: Using a single hidden layer neural network as a decoder enables learning the degree of relationship between input entities even though far fewer parameters are employed for learning ( $\mathbf{k}$  and  $\mathbf{u}$ ) compared to conventional neural tensor networks (hidden output layers in Fig. 1).

### RWTNs with Weight Sharing

A unique feature of RWTNs is that because the weights of the randomized NTN encoder are independent of the training data, the encoder network can be shared among decoder networks trained for different classifiers. We refer to this property as *weight sharing*. Fig. 2 shows a visualization of the structure of our model applied with weight sharing to the learning of  $i$  different classifiers. The large dashed box surrounds a single encoder network that serves as a common feature extractor for all classifiers. Instead of generating the encoder network for each classifier (as in a conventional LTN), each classifier uses the same encoder network, and training only requires learning the weights of that classifier’s relatively simple decoder network. This approach

increases reusability and cost efficiency in a way that goes beyond what is possible with LTNs which must train all encoder and decoder networks separately for each classifier.

### Experimental Evaluation

To evaluate the performance of our proposed RWTNs over LTNs, we employ both for Semantic Image Interpretation (SII) tasks, which extract structured semantic descriptions from images. Very few SRL applications have been applied to SII tasks because of the high complexity involved with image learning. Donadello, Serafini, and Garcez (2017) define two main tasks of SII as: (i) the classification of bounding boxes, and (ii) the detection of the *part-of* relation between any two bounding boxes. They demonstrated that LTNs can successfully improve the performance of solely data-driven approaches, including the state-of-the art Fast Region-based Convolutional Neural Networks (Fast R-CNN) (Girshick 2015). Our experiments are conducted by comparing the performance of two tasks of SII between RWTNs and LTNs. These tasks are well defined in first-order logic, and the codes implemented in TENSORFLOW<sup>TM</sup> have been provided and thus can be easily used to compare the performance of LTNs with RWTNs.

### Methods

We provide details of our experimental comparison of RTWns and LTNs. In this section, we introduce (i) how to formalize our two focal SII tasks in FOL grounded in RWTNs and LTNs, (ii) the data set used in the test, and (iii) the RWTN and LTN hyperparameters used in the test.

**Formalizing SII in First-Order Logic:** A signature  $\Sigma_{SII} = \langle \mathcal{C}, \mathcal{F}, \mathcal{P} \rangle$  is defined where  $\mathcal{C} = \bigcup_{p \in P_{ics}} b(p)$  is the set of identifiers for all the bounding boxes in all the images,  $\mathcal{F} = \emptyset$ , and  $\mathcal{P} = \{\mathcal{P}_1, \mathcal{P}_2\}$ , where  $\mathcal{P}_1$  is a set of unary predicates, one for each object type (e.g.,  $\mathcal{P}_1 = \{\text{Dog}, \text{Tail}, \dots\}$ ), and  $\mathcal{P}_2$  is a set of binary predicates representing relations between objects. Because our experiments focus on the *part-of* relation,  $\mathcal{P}_2 = \{\text{partOf}\}$ . The FOL formulas based on this signature can specify: (i) simple facts; the fact that  $b$  contains either a cat or a dog, or (ii) general rules.

We define the grounding for  $\Sigma_{SII}$  such that each constant  $b$ , indicating a bounding box, is associated with geometric features describing the position and the dimension of the bounding box and semantic features indicating the classification score returned by the bounding box detector for each class. For example, for each bounding box  $b \in \mathcal{C}, C_i \in \mathcal{P}_i, \mathcal{G}(b)$  is the  $\mathbb{R}^{4+|\mathcal{P}_1|}$  vector:

$$\langle \text{class}(C_1, b), \dots, \text{class}(C_{|\mathcal{P}_1|}, b), \dots, x_0(b), y_0(b), x_1(b), y_1(b) \rangle$$

where the last four features are the coordinates of the top-left and bottom-right corners of  $b$ , and  $\text{class}(C_i, b) \in [0, 1]$  is the classification score of the bounding box detector for  $b$ . For each class  $C_i \in \mathcal{P}_1$ , define the grounding:

$$\mathcal{G}(C_i)(\mathbf{x}) = \begin{cases} 1, & \text{if } i = \arg \max_{1 \leq l \leq |\mathcal{P}_1|} x_l \\ 0 & \text{otherwise} \end{cases} \quad (6)$$

where  $\mathbf{x} = \langle x_1, \dots, x_{4+|\mathcal{P}_1|} \rangle$  is the vector corresponding to the grounding of a bounding box.

$\mathcal{G}(\text{partOf}(b, b'))$  can be defined as:

$$\begin{cases} 1, & \text{if } ir(b, b') \cdot \max_{i,j=1}^{|\mathcal{P}_1|} (w_{ij} \cdot x_i \cdot x'_j) \geq th_{ir} \\ 0 & \text{otherwise} \end{cases} \quad (7)$$

for some threshold  $th_{ir}$  (usually,  $th_{ir} > 0.5$ ) where  $ir(b, b') = \frac{\text{area}(b \cap b')}{\text{area}(b)}$  and  $w_{ij} = 1$  if  $C_i$  is a part of  $C_j$  ( $w_{ij} = 0$  otherwise). Given the above grounding, we can compute the grounding of any atomic formula thus expressing the degree of truth of the formula.

### Defining the Grounded Theories for RWTNs and LTNs:

A suitable ground theory  $GT$  can be built for SII. Let  $Pics^t \subseteq Pics$  be a set of bounding boxes of images correctly labelled with the classes that they belong to, and let each pair of bounding boxes be correctly labelled with the *part-of* relation. Then,  $Pics^t$  can be considered as a training set and a grounded theory  $\mathcal{T}_{LTN}$  can be constructed as follows:  $\mathcal{T}_{LTN} = \langle \mathcal{K}, \hat{\mathcal{G}} \rangle$ , where:

- $\mathcal{K}$  contains: (i) the set of closed literals  $C_i(b)$  and  $\text{partOf}(b, b')$  for every bounding box  $b$  labelled with  $C_i$  and for every pair of bounding boxes  $\langle b, b' \rangle$  connected by the *partOf* relation, and (ii) the set of the mereological constraints for the *part-of* relation, including asymmetric constraints, lists of several parts of an object, or restrictions that whole objects cannot be part of other objects and every part object cannot be divided further into parts.
- The partial grounding  $\hat{\mathcal{G}}$  is defined on all bounding boxes of all the images in  $Pics$  where both  $\text{class}(C_i, b)$  and the bounding box coordinates are computed by the Fast RCNN object detector.  $\hat{\mathcal{G}}$  is not defined for the predicate symbols in  $\mathcal{P}$  and is to be learned.

A grounded theory  $\mathcal{T}_{RWTN}$  is only slightly different.  $\mathcal{T}_{RWTN} = \langle \mathcal{K}, \hat{\mathcal{G}}_{rwtN} \rangle$  where a partial grounding  $\hat{\mathcal{G}}_{rwtN}$  can be described for predicates using eq.(5). Thus, we can easily compare the performance between  $\hat{\mathcal{G}}_{rwtN}$  and  $\hat{\mathcal{G}}$ .

**Datasets:** The PASCAL-PART-dataset (Chen et al. 2014) and ontologies (WORDNET) are chosen for the *part-Of* relation. The PASCAL-PART-dataset contains 10103 images with bounding boxes. They are annotated with object-types and the part-of relation defined between pairs of bounding boxes. There are three main groups in labels—animals, vehicles, and indoor objects—with their corresponding parts and “part-of” label. There are 59 labels (20 labels for whole objects and 39 labels for parts). The images were then split into a training set with 80% of the images and a test set with 20% of the images, maintaining the same proportion of the number of bounding boxes for each label. Given a set of bounding boxes detected by an object detector (Fast-RCNN), the task of object classification is to assign to each bounding box an object type. The task of *part-Of* detection is to decide, given two bounding boxes, if the object contained in the first is a part of the object contained in the second.

**Hyperparameter Setting:** To compare the performance between RWTNs and LTNs, we train two models separately.

- For RWTN, the spectral radius  $\rho$  is set to 0.6, the connection sparsity  $\beta$  is 0.25. The size of the reservoir  $R$  is 200. The input scaling  $\omega$  is 0.5. The noise level  $\xi$  is 0.01. The number of hidden units for a readout  $t$  is 20.
- For LTN, we configure the experimental environment following Donadello, Serafini, and Garcez (2017). The LTNs were configured with a tensor of  $k = 6$  layers.

Both models make use of a regularization parameter  $\lambda = 10^{-10}$ , Lukasiewicz’s  $t$ -norm ( $\mu(a, b) = \max(0, a + b - 1)$ ), and the harmonic mean as an aggregation operator. We ran 1000 training epochs of the RMSProp learning algorithm available in TENSORFLOW<sup>TM</sup> for each model.

### Results

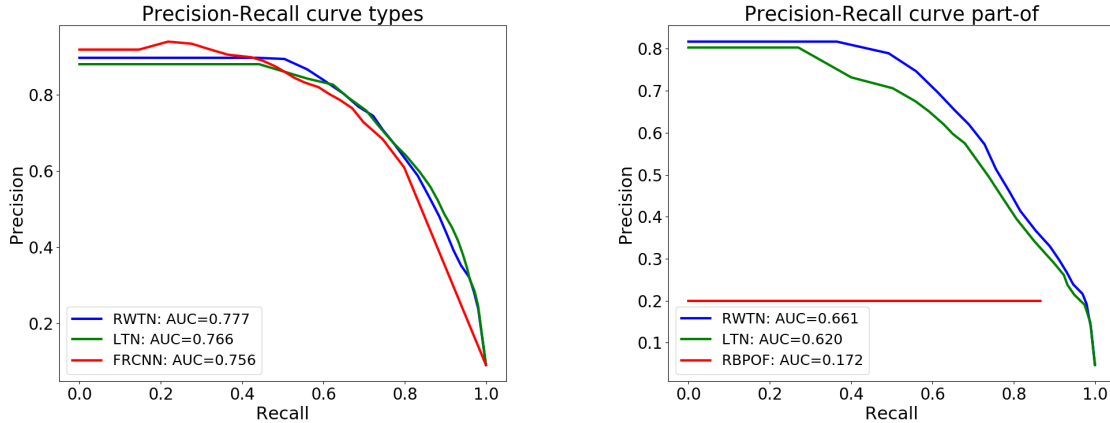
Our experiments mainly focus on the comparison of the performance between our model and LTN, but figures also include the results with the Fast-RCNN (Girshick 2015) at type classification (Eq. (6)) and the inclusion ratio  $ir$  baseline (Eq. (7)) at the *part-Of* detection task. If  $ir$  is greater than a given threshold  $th$  (in our experiments,  $th = 0.7$ ), then the bounding boxes are said to be in the *partOf* relation. Every bounding box  $b$  is classified into  $C \in \mathcal{P}_1$  if  $\mathcal{G}(C(b)) > th$ .

Results for indoor objects are shown in Fig. 3 where AUC is the area under the precision–recall curve. The results show that, for the *part-Of* relation and object types classification, RWTNs achieve better performance than LTNs. However, there are some variance in the results because of the stochastic nature of the experiments. Consequently, we carried out five such experiments for each task, for which the sample averages and 95% confidence intervals are shown in Table 1. These results confirm that our model can achieve similar performance as LTNs for object-task classification and superior performance for detection of *part-of* relations.

In Table 1, we only included AUC numbers for RWTNs with weight sharing (third column) for object-type classification because *part-of* relations only require a single classifier. The performance of RWTNs with weight sharing for the object-type classification task (which requires 11 classifiers for indoor objects, 23 for vehicles, and 26 for animals) shows only a marginal gap in performance compared to other models, which demonstrates the effectiveness and efficiency of the approach of using a shared, randomized NTN in RWTNs with weight sharing.

### Relative Complexity of RWTNs and LTNs

To better appreciate the relative performance of RWTNs and LTNs, we can compare the number of parameters to learn for grounding a unary predicate for each model. Let  $n$  be the number of features of an input ( $n = 64$ ) for both RWTNs and LTNs. As shown in Eq. (4), the parameters to learn in LTNs are  $\{u_P \in \mathbb{R}^k, W_P^{[1:k]} \in \mathbb{R}^{n \times n \times k}, V_P \in \mathbb{R}^{k \times n}, b_P \in \mathbb{R}^k\}$ , where  $k = 6$  following the configuration of the LTNs. Thus, the number of parameters in LTNs is  $(n^2 + n + 2) \cdot k = (64^2 + 64 + 2) \cdot 6 = 24972$ .



(a) RWTNs sometimes outperform LTNs on object type classification, achieving an Area Under the Curve (AUC) of 0.777 in comparison with 0.766. (b) RWTNs mostly show better performance than LTNs in the detection of *part-of* relations, achieving AUC of 0.661 in comparison with 0.620.

Figure 3: Precision–recall curves for indoor objects type classification and the *partOf* relation between objects.

On the other hand, in Eq. (5), the learnable parameters in RWTNs are only  $\{\mathbf{k} \in \mathbb{R}^t, u \in \mathbb{R}^{R \times t}\}$ , where  $R = 200$  and  $t = 20$  following the configuration of the RWTNs. Therefore, the number of learnable parameters in RWTNs is  $(R+1) \cdot t = 201 \cdot 20 = 4020$ . The fact that the number of parameters to learn in RWTNs (4020) is significantly smaller compared to LTNs (24972) shows that non-adaptable parameters in RWTNs can have significant power to represent the latent relationship among objects so that the model can efficiently extract relational knowledge even though using fewer parameters. Furthermore, the number of the parameters of LTNs heavily depends on the number of features, whereas RWTNs are independent of the number of features. In principle, this could allow the learning process in our model to be accelerated if the feature representation from the encoder model is pre-processed and stored.

### Space Complexity of RWTNs with Weight Sharing

Weight sharing is a unique feature of RWTNs, which can greatly reduce necessary space complexity when multiple classifiers are used simultaneously. In the depicted case of

Table 1: AUC of T1 (object type classification) and T2 (detection of *part-of* relation) for LTN, RWTN, and RWTN with weight sharing across label groups

LABEL	TASKS	LTN	RWTN	RWTN w/ W.S
INDOOR	T1	<b>.77 ± .027</b>	<b>.77 ± .012</b>	.76 ± .0068
	T2	.64 ± .060	<b>.66 ± .049</b>	-
VEHICLE	T1	<b>.73 ± .017</b>	.71 ± .030	.70 ± .014
	T2	.53 ± .065	<b>.58 ± .037</b>	-
ANIMAL	T1	<b>.69 ± .028</b>	<b>.69 ± .024</b>	.68 ± .016
	T2	.60 ± .092	<b>.64 ± .070</b>	-

learning  $i$  classifiers in Fig. 2, space complexity for RWTNs is  $((n^2 + n) \cdot R + (R + 1) \cdot t) \cdot i \approx O(iRn^2)$ . However, with weight sharing, RWTNs can achieve much better space complexity, which is  $(n^2 + n) \cdot R + (R + 1) \cdot t \cdot i \approx O(Rn^2)$  because  $i \cdot t < n^2$  for the experiments conducted in the SII task. This indicates that the number of classifiers can have a negligible effect on the spatial complexity of RWTNs when weight sharing is used.

### Conclusion and Future Work

In this paper, we introduced Randomly Weighted Tensor Networks, which, when compared to a conventional neural tensor model, act as a generalized feature extractor with greater relational expressiveness and a learning model with relatively simpler structure. We demonstrated how insights from Reservoir Computing normally reserved for time-series analysis can be applied to the fields of neural-symbolic computing and knowledge representation and reasoning for relational learning.

Our work can be advanced in several ways. We will investigate how other methods from reservoir computing for exploring efficient reservoir topologies (Ferreira and Luder-mir 2009; Sun et al. 2017; Wang, Jin, and Hao 2019) might be generalized to these new application spaces. In addition, we shall extend RWTNs to include a recurrent part for representing dynamic features of time-series data; this approach may allow for extracting time-varying relational knowledge necessary for developing a framework for data-driven reasoning over temporal logic. In addition, ensemble learning may be able to capitalize on blending across RWTNs with different random realizations.

### Acknowledgments

Funding was provided by contract number FA8651-17-F-1013 from the USAF/Eglin AFB/FL contract number

## References

- Bergmann, M. 2008. *An introduction to many-valued and fuzzy logic: semantics, algebras, and derivation systems*. Cambridge University Press.
- Bianchi, F. M.; De Santis, E.; Rizzi, A.; and Sadeghian, A. 2015a. Short-term electric load forecasting using echo state networks and PCA decomposition. *IEEE Access* 3: 1931–1943.
- Bianchi, F. M.; Livi, L.; and Alippi, C. 2016. Investigating echo-state networks dynamics by means of recurrence analysis. *IEEE transactions on neural networks and learning systems* 29(2): 427–439.
- Bianchi, F. M.; Scardapane, S.; Løkse, S.; and Jenssen, R. 2018. Reservoir computing approaches for representation and classification of multivariate time series. *arXiv preprint arXiv:1803.07870*.
- Bianchi, F. M.; Scardapane, S.; Uncini, A.; Rizzi, A.; and Sadeghian, A. 2015b. Prediction of telephone calls load using echo state network with exogenous variables. *Neural Networks* 71: 204–213.
- Bordes, A.; Weston, J.; Collobert, R.; and Bengio, Y. 2011. Learning structured embeddings of knowledge bases. In *Twenty-Fifth AAAI Conference on Artificial Intelligence*.
- Chen, X.; Mottaghi, R.; Liu, X.; Fidler, S.; Urtasun, R.; and Yuille, A. 2014. Detect what you can: Detecting and representing objects using holistic models and body parts. In *Proceedings of the IEEE Conference on Computer Vision and Pattern Recognition*, 1971–1978.
- Deihimi, A.; and Showkati, H. 2012. Application of echo state networks in short-term electric load forecasting. *Energy* 39(1): 327–340.
- Donadello, I.; Serafini, L.; and Garcez, A. D. 2017. Logic tensor networks for semantic image interpretation. *arXiv preprint arXiv:1705.08968*.
- Ferreira, A. A.; and Ludermir, T. B. 2009. Genetic algorithm for reservoir computing optimization. In *2009 International Joint Conference on Neural Networks*, 811–815. IEEE.
- Garcez, A. S.; Lamb, L. C.; and Gabbay, D. M. 2008. *Neural-symbolic cognitive reasoning*. Springer Science & Business Media.
- Girshick, R. 2015. Fast r-cnn. In *Proceedings of the IEEE international conference on computer vision*, 1440–1448.
- Guha, R. 2015. Towards a model theory for distributed representations. In *2015 AAAI Spring Symposium Series*.
- Jaeger, H. 2001. The “echo state” approach to analysing and training recurrent neural networks-with an erratum note. *Bonn, Germany: German National Research Center for Information Technology GMD Technical Report* 148(34): 13.
- Koller, D.; Friedman, N.; Džeroski, S.; Sutton, C.; McCallum, A.; Pfeffer, A.; Abbeel, P.; Wong, M.-F.; Heckerman, D.; Meek, C.; et al. 2007. *Introduction to statistical relational learning*. MIT press.
- Nath, A.; and Domingos, P. M. 2015. Learning relational sum-product networks. In *Twenty-Ninth AAAI Conference on Artificial Intelligence*.
- Nickel, M.; Murphy, K.; Tresp, V.; and Gabrilovich, E. 2015. A review of relational machine learning for knowledge graphs. *Proceedings of the IEEE* 104(1): 11–33.
- Pearl, J. 2014. *Probabilistic reasoning in intelligent systems: networks of plausible inference*. Elsevier.
- Richardson, M.; and Domingos, P. 2006. Markov logic networks. *Machine learning* 62(1-2): 107–136.
- Rodan, A.; Sheta, A. F.; and Faris, H. 2017. Bidirectional reservoir networks trained using SVM+privileged information for manufacturing process modeling. *Soft Computing* 21(22): 6811–6824.
- Rodan, A.; and Tino, P. 2010. Minimum complexity echo state network. *IEEE transactions on neural networks* 22(1): 131–144.
- Santoro, A.; Raposo, D.; Barrett, D. G.; Malinowski, M.; Pascanu, R.; Battaglia, P.; and Lillicrap, T. 2017. A simple neural network module for relational reasoning. In *Advances in neural information processing systems*, 4967–4976.
- Scardapane, S.; and Wang, D. 2017. Randomness in neural networks: an overview. *Wiley Interdisciplinary Reviews: Data Mining and Knowledge Discovery* 7(2): e1200.
- Serafini, L.; and Garcez, A. d. 2016. Logic tensor networks: Deep learning and logical reasoning from data and knowledge. *arXiv preprint arXiv:1606.04422*.
- Socher, R.; Chen, D.; Manning, C. D.; and Ng, A. 2013. Reasoning with neural tensor networks for knowledge base completion. In *Advances in neural information processing systems*, 926–934.
- Sun, X.; Li, T.; Li, Q.; Huang, Y.; and Li, Y. 2017. Deep belief echo-state network and its application to time series prediction. *Knowledge-Based Systems* 130: 17–29.
- Sutskever, I.; and Hinton, G. E. 2009. Using matrices to model symbolic relationship. In *Advances in neural information processing systems*, 1593–1600.
- Wang, J.; and Domingos, P. M. 2008. Hybrid Markov Logic Networks. In *AAAI*, volume 8, 1106–1111.
- Wang, X.; Jin, Y.; and Hao, K. 2019. Echo state networks regulated by local intrinsic plasticity rules for regression. *Neurocomputing* 351: 111–122.